Supporting Information

Selective oxidation of CH_4 to HCHO over defective $rTiO_2$/GO metal-free photocatalyst

Yingdong Hao[1, 2, #], Fang Mao[1, #], Yonghui Zhao[1], Nannan Sun[1, *], Wei Wei[1, 3, *]

[1] CAS Key Lab of Low-Carbon Conversion Science and Engineering, Shanghai Advanced Research Institute, Chinese Academy of Sciences, Shanghai 201210, China

[2] University of Chinese Academy of Sciences, Beijing 100049, China

[3] School of Physical Science and Technology, ShanghaiTech University, Shanghai 201210, China

[#] These authors contributed equally

[*] Corresponding Author

E-mail address: sunnn@sari.ac.cn, weiwei@sari.ac.cn

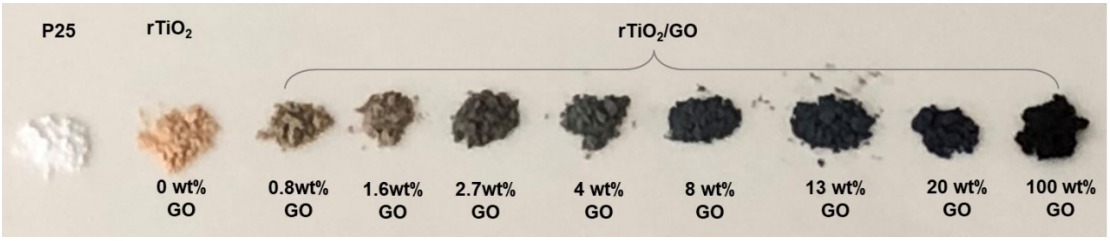

Fig. S1 Photographs of TiO_2 (P25) and the $rTiO_2$/*x*GO photocatalysts.

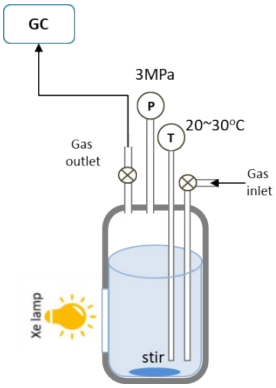

Fig. S2 Schematic diagram of the photocatalytic reaction system.

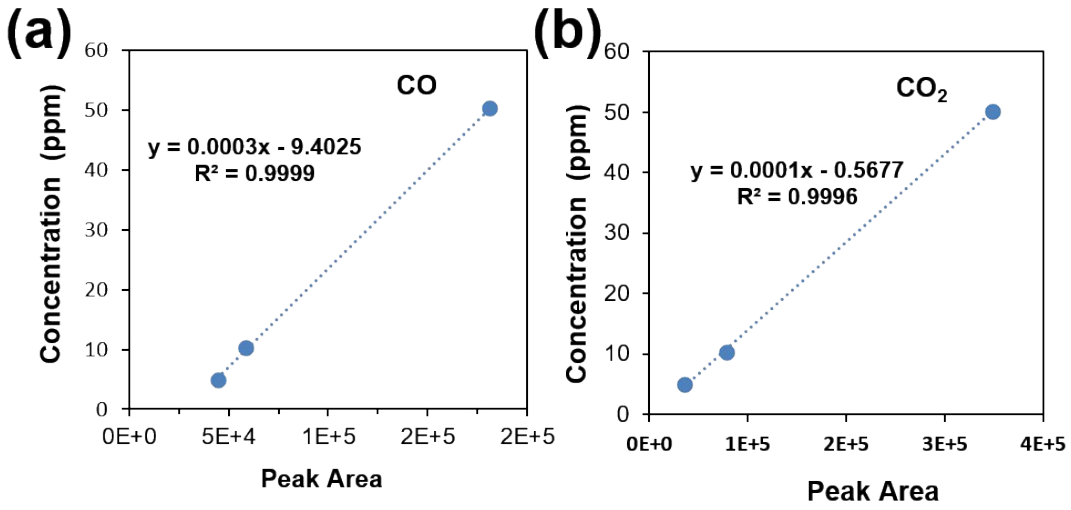

Fig. S3 Calibration curve for GC quantification of (a) CO and (b) CO_2.

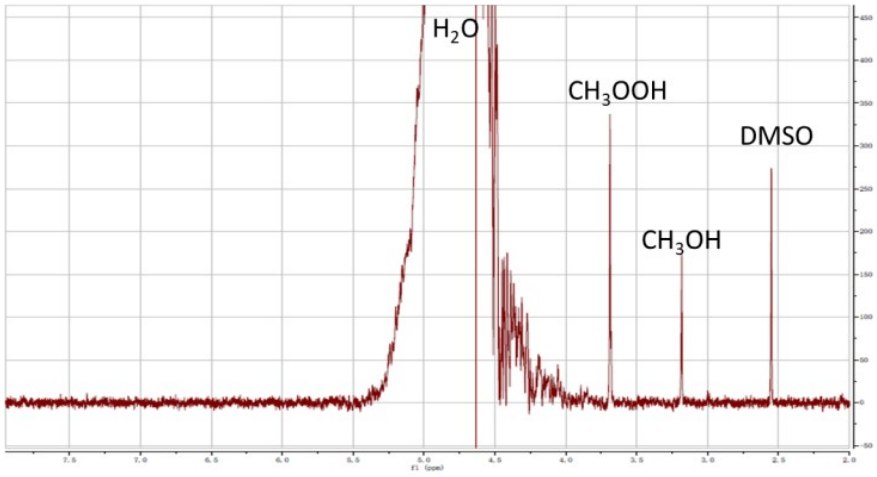

Fig. S4 Typical ^{1}H NMR spectrum of the liquid products.

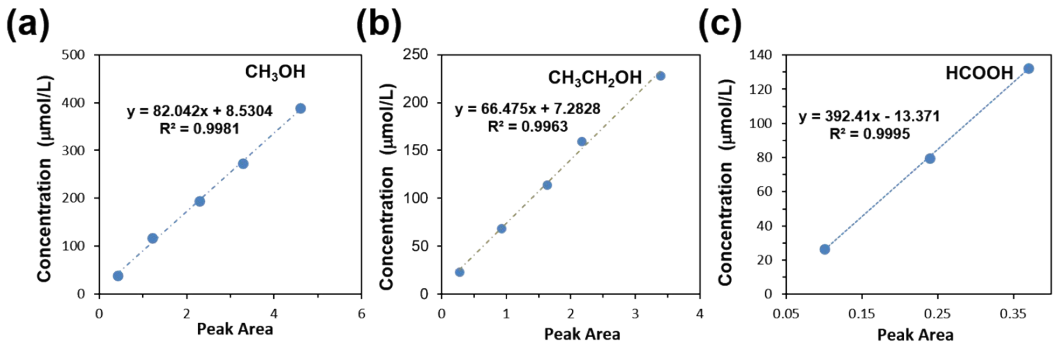

Fig. S5 ^{1}H NMR calibration curves for (a) CH_3OH, (b) CH_3CH_2OH, and (c) HCOOH. As the protons of methyl in CH_3OH and CH_3OOH molecules is same, quantification of CH_3OOH is calibrated by the same curve as that of CH_3OH.

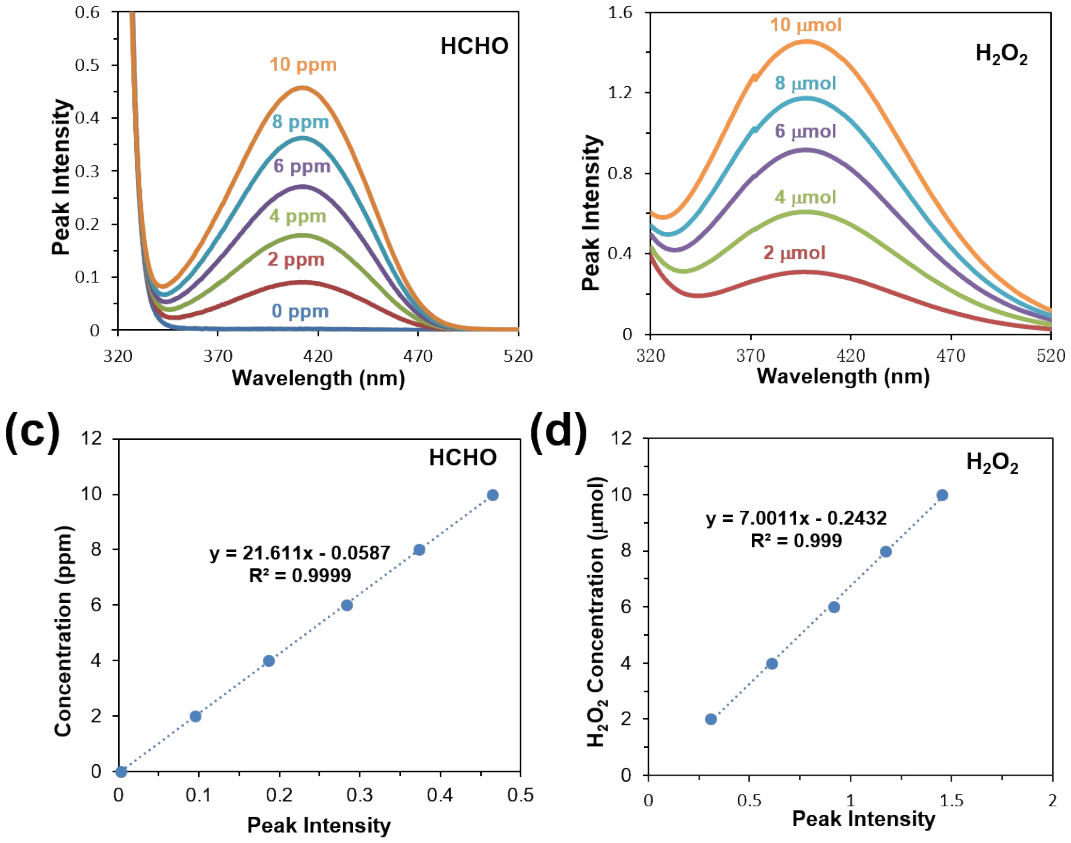

40

41 **Fig. S6** Analysis of HCHO and H_2O_2 by UV-Vis spectra. UV-Vis absorption spectra (a) HCHO
42 and (b) H_2O_2. Calibration curves for (c) HCHO and (d) H_2O_2.

43

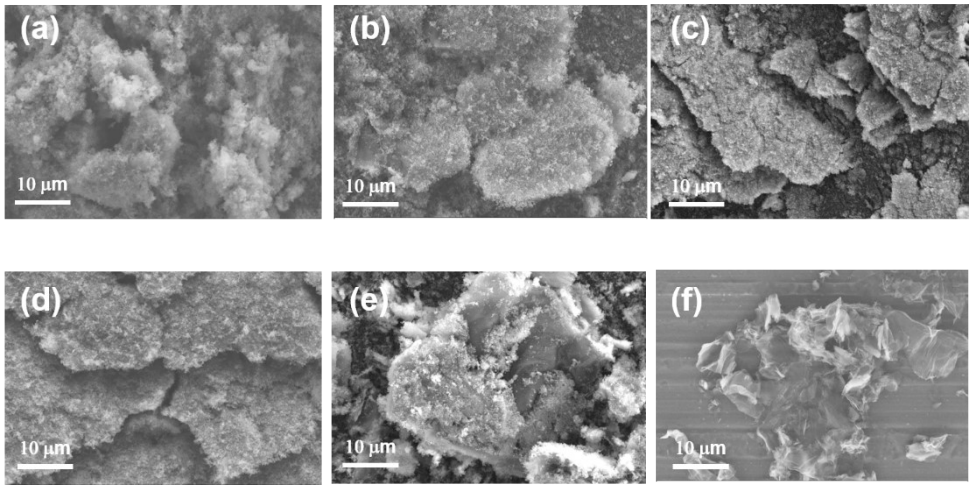

Fig. S7 SEM images. (a) $rTiO_2$, (b) $rTiO_2$/0.8GO, (c) $rTiO_2$/2.7GO, (d) $rTiO_2$/4.0GO, (e) $rTiO_2$/20.0GO, and (f) GO.

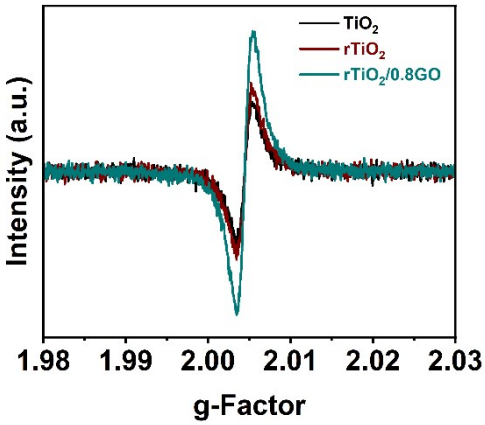

Fig. S8 EPR spectra.

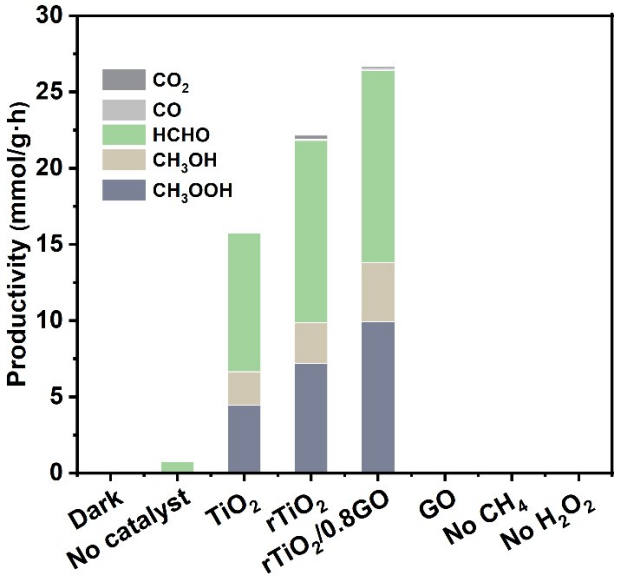

Fig. S9 Photocatalytic oxidation of CH_4 at different conditions.

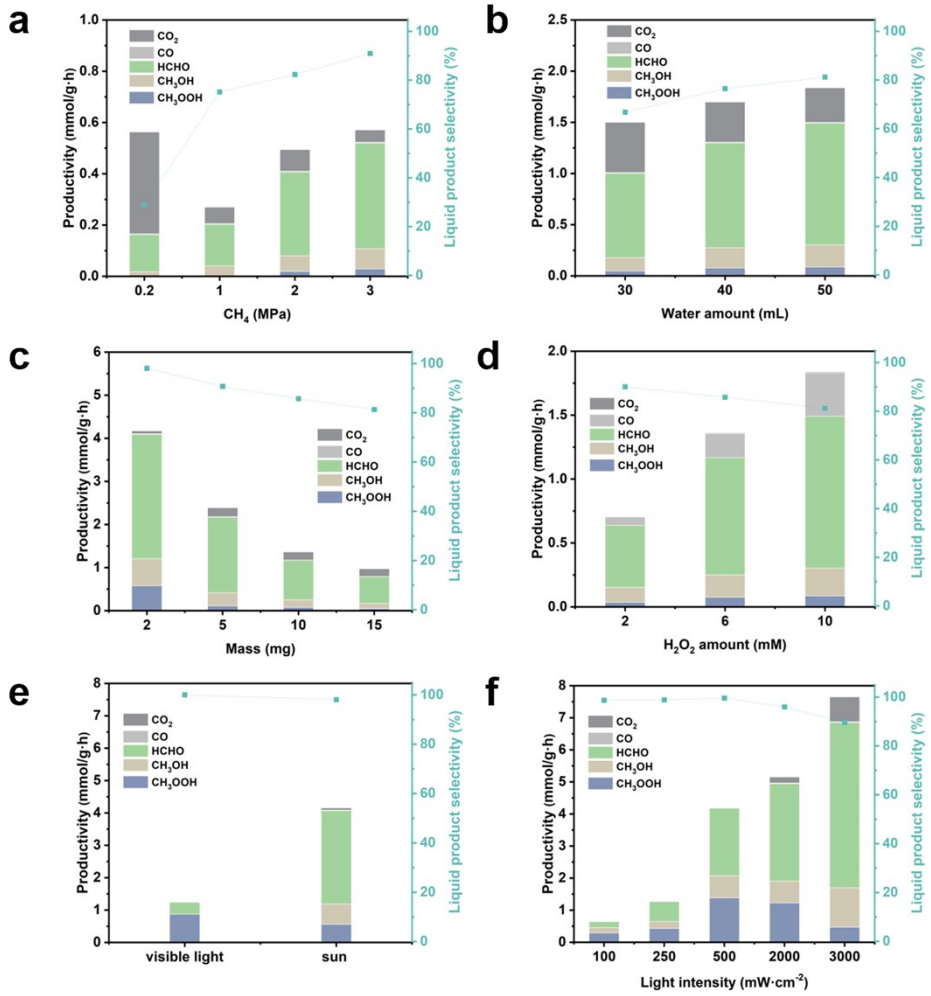

Fig. S10 Effect of (a) CH_4 pressure, (b) H_2O volume, (c) catalyst weight, (d) H_2O_2 dosage, (e) light source (f) light intensity.

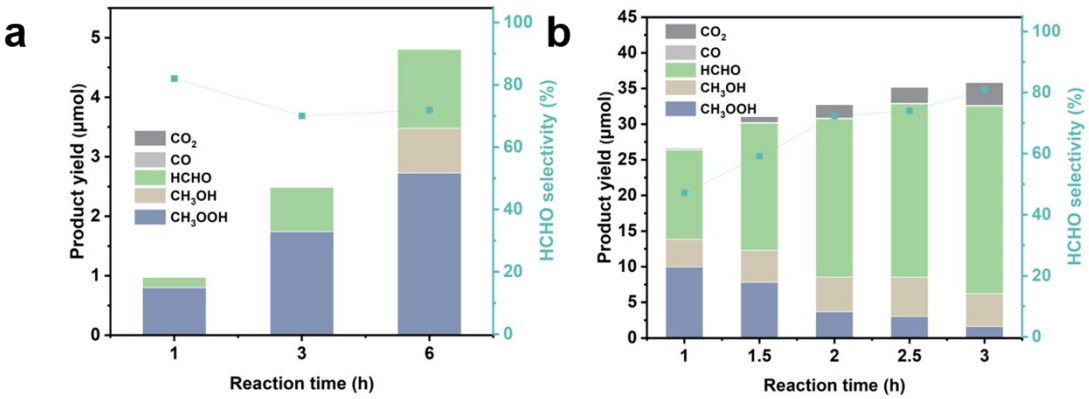

Fig. S11 Photocatalytic oxidation of CH_4 under (a) visible light and (b) sun light.

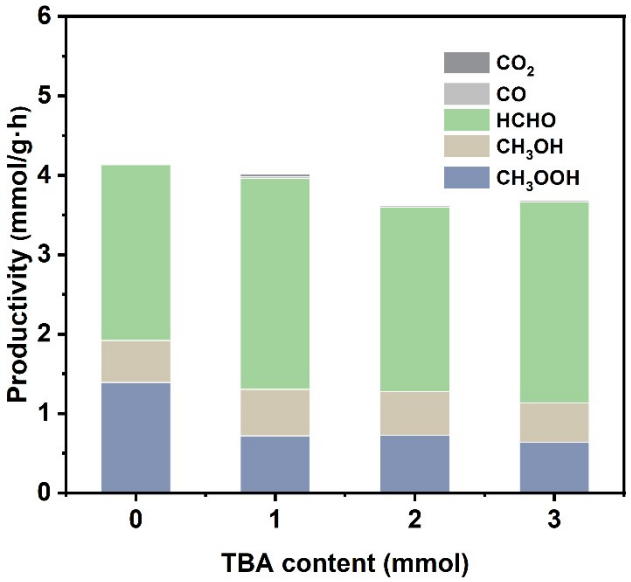

Fig. S12 •OH quenching with different TBA content.

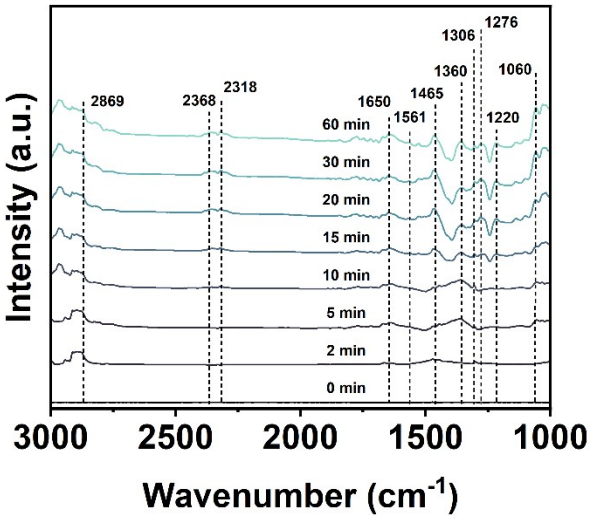

Fig. S13 In situ FTIR spectra for CH_4 photooxidation over the $rTiO_2$/0.8GO during light irradiation time from 0 to 60 min.

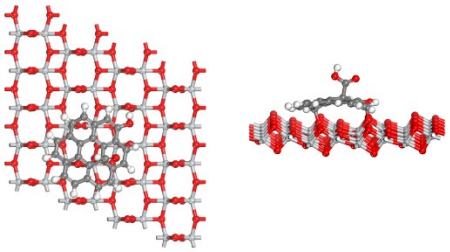

Fig. S14 Top and side views of the TiO_2(101)/GO surface. (Dark gray: C; light gray: C; red: O; white: H).

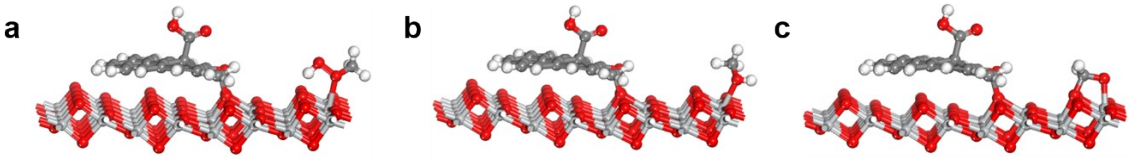

Fig. S15 Side views of the optimized geometries of C1-oxygenates adsorption on the TiO_2/GO surfaces. (a) CH_3OOH, (b) CH_3OH, (c) CH_2O. (Dark gray: C; light gray: C; red: O; white: H).

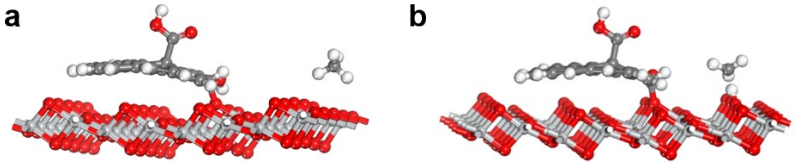

Fig. S16 (a) CH_4 adsorption structure and (b) CH_4 dissociation transition states on the TiO_2(101)/GO surface. (Dark gray: C; light gray: C; red: O; white: H).

A large p(4×5) supercell of the rTiO_2(101) surface with the GO cluster was built to model the rTiO_2/GO system (Fig. S14)[2]. From van der Waals (vdW) corrected density functional theory (DFT) calculation, it was found that the most stable adsorption sites of C1-oxygeantes (CH_3OOH*, CH_3OH* and CH_2O*) were the Ti atom sites (Fig. S15). Furthermore, CH_4 dissociation preferably happened on the lattice oxygen of TiO_2(101) surface, and the process is thermodynamically prohibited on GO (Fig. S16a and b). Therefore, it was deduced that GO may have little in direct activation of CH_4. In the revised manuscript, the above results and discussion are added.